PNAS RESEARCH ARTICLE | MICROBIOLOGY

The ZCCHC14/TENT4 complex is required for hepatitis A virus RNA synthesis

You Li[a,b,1], Ichiro Misumi[a,c,1], Tomoyuki Shiota[a], Lu Sun[a], Erik M. Lenarcic[d], Hyejeong Kim[d], Takayoshi Shirasaki[a], Adriana Hertel-Wulff[a], Taylor Tibbs[c,d], Joseph E. Mitchell[c,d], Kevin L. McKnight[a], Craig E. Cameron[a,d], Nathaniel J. Moorman[a,d], David R. McGivern[a,b,2], John M. Cullen[e], Jason K. Whitmire[a,c,d], and Stanley M. Lemon[a,b,d,3]

Edited by Peter Sarnow, Stanford University School of Medicine, Stanford, CA; received March 21, 2022; accepted May 13, 2022

Despite excellent vaccines, resurgent outbreaks of hepatitis A have caused thousands of hospitalizations and hundreds of deaths within the United States in recent years. There is no effective antiviral therapy for hepatitis A, and many aspects of the hepatitis A virus (HAV) replication cycle remain to be elucidated. Replication requires the zinc finger protein ZCCHC14 and noncanonical TENT4 poly(A) polymerases with which it associates, but the underlying mechanism is unknown. Here, we show that ZCCHC14 and TENT4A/B are required for viral RNA synthesis following translation of the viral genome in infected cells. Cross-linking immunoprecipitation sequencing (CLIP-seq) experiments revealed that ZCCHC14 binds a small stem-loop in the HAV 5′ untranslated RNA possessing a Smaug recognition-like pentaloop to which it recruits TENT4. TENT4 polymerases lengthen and stabilize the 3′ poly(A) tails of some cellular and viral mRNAs, but the chemical inhibition of TENT4A/B with the dihydroquinolizinone RG7834 had no impact on the length of the HAV 3′ poly(A) tail, stability of HAV RNA, or cap-independent translation of the viral genome. By contrast, RG7834 inhibited the incorporation of 5-ethynyl uridine into nascent HAV RNA, indicating that TENT4A/B function in viral RNA synthesis. Consistent with potent in vitro antiviral activity against HAV (IC_{50} 6.11 nM), orally administered RG7834 completely blocked HAV infection in *Ifnar1*$^{-/-}$ mice, and sharply reduced serum alanine aminotransferase activities, hepatocyte apoptosis, and intrahepatic inflammatory cell infiltrates in mice with acute hepatitis A. These results reveal requirements for ZCCHC14-TENT4A/B in hepatovirus RNA synthesis, and suggest that TENT4A/B inhibitors may be useful for preventing or treating hepatitis A in humans.

picornavirus | antiviral therapy | animal model | hepatitis A | RNA-binding protein

Significance

Despite excellent vaccines, unprecedented outbreaks of hepatitis A have resulted in more than 400 fatal infections in the United States since 2016. Many gaps exist in our current understanding of the responsible pathogen, hepatitis A virus (HAV), for which there are no available antiviral therapies. Here, we show how the RNA genome of this unique, hepatotropic picornavirus interacts with a host cell protein complex required for synthesis of the viral RNA. We demonstrate that targeting this complex with an orally delivered small-molecule therapeutic ablates viral replication and reverses liver inflammation in a mouse model of hepatitis A, providing proof-of-principle for antiviral therapy and showing the potential for chemoprevention of hepatitis A in outbreak settings.

Although the incidence of acute hepatitis A declined dramatically in the United States following the introduction of inactivated vaccines in 1995, widespread community outbreaks in recent years have led to an unprecedented resurgence of the virus, with more than 23,000 hospitalizations and more than 400 deaths since 2016 (1–3). No effective treatment exists for the liver injury caused by hepatitis A virus (HAV), an atypical hepatotropic picornavirus that spreads by fecal–oral transmission (4). Other than orthotopic liver transplantation, which may be lifesaving in patients with fulminant hepatitis A, there have been no advances in the treatment of this infection since discovery of the virus half a century ago. HAV is distinct from other picornaviruses in its phylogeny, structure, and replication strategy (5, 6). It infects the liver in a stealth-like manner, releasing newly replicated virus into the gastrointestinal tract through the biliary system (7, 8). Replication is noncytopathic and restricted to hepatocytes. Newly replicated virus is released without lysis from cells within small extracellular vesicles resembling exosomes (9). These membrane-cloaked "quasi-enveloped" virions are infectious and the only form of the virus detected in blood during acute hepatitis A (9, 10). Acute liver injury is caused by both adaptive and innate immune responses to infection, with both B and T cell responses involved in control of the virus (11–14).

Although many aspects of the viral replication cycle remain unstudied, recent genome-wide CRISPR screens have identified a variety of host cell factors required for HAV infection (15, 16). Among others, these include enzymes mediating the synthesis of gangliosides, which function as endosomal receptors for the virus, numerous proteins involved in cap-independent translation of the viral genome, and the zinc finger RNA-binding protein ZCCHC14 (15, 16). Replication also requires the noncanonical poly(A) polymerases TENT4A/B, with which ZCCHC14 is known to associate (16, 17), and can be inhibited by the dihydroquinolizinone TENT4A/B inhibitor, RG7834 (16, 18). The mechanism underlying this requirement for ZCCHC14 and TENT4A/B remains obscure. Here, we show that ZCCHC14 binds a small stem-loop in the 5′ untranslated

Y.L. and S.M.L. are co-inventors on a patent application related to DHQ-E-OH. The other authors declare no competing interest.

This article is a PNAS Direct Submission.

[1]Y.L. and I.M. contributed equally to this work.

[2]Present address: Center for Biologics Evaluation and Research, Food and Drug Administration, Silver Spring, MD 20993.

[3]To whom correspondence may be addressed. Email: smlemon@med.unc.edu.

This article contains supporting information online at http://www.pnas.org/lookup/suppl/doi:10.1073/pnas.2204511119/-/DCSupplemental.

Published July 7, 2022.

RNA (5′ UTR) segment of the genome to which it recruits TENT4A, and that the recruitment of ZCCHC14-TENT4 is essential for a step in viral RNA synthesis. We also show that orally administered RG7834 potently blocks viral replication and interrupts pathogenesis in *Ifnar1*$^{-/-}$ mice with acute hepatitis A, suggesting that chemical inhibitors of TENT4 may be useful in the treatment and prevention of hepatitis A in humans.

Rsults

The ZCCHC14/TENT4 Complex Is Required for HAV RNA Synthesis. Genome-wide CRISPR screens by us and others identified ZCCHC14 as an essential host factor for HAV infection in cultured hepatoma cells (*SI Appendix*, Fig. S1 *A* and *B*) (15, 16). Consistent with this, targeted knockout of ZCCHC14 in Huh-7.5 cells (ZCCHC14-KO [knockout] cells) ablated the replication of a low-passage, cell culture–adapted virus (HM175 p16) (19) (Fig. 1 *A*–*C*) as well as a highly cell culture–adapted subgenomic replicon RNA lacking capsid sequence (18f-Fluc) (20) (Fig. 1 *A* and *D*). Replication of a recombinant reporter virus (18f-NLuc) (21) (Fig. 1*A*) was also impaired in ZCCHC14-KO cells, and in 293T cells with small interfering RNA (siRNA)-mediated ZCCHC14 depletion, further confirming the requirement for ZCCHC14 (*SI Appendix*, Fig. S1 *C* and *D*). Replication was rescued in the 293T cells by restoring ZCCHC14 expression (*SI Appendix*, Fig. S1*E*). By contrast, a luciferase-expressing poliovirus replicon replicated well in ZCCHC14-KO cells (*SI Appendix*, Fig. S1*F*), indicating that ZCCHC14 is not universally required by picornaviruses.

Importantly, the amount of NLuc expressed by the 18f-NLuc reporter virus was not reduced by ZCCHC14 KO at 4 h postinfection (p.i.), which is before new viral RNA synthesis (22) (Fig. 1*E*). Similarly, ZCCHC14 KO did not impair NLuc expressed following the electroporation of a mutated, replication-incompetent 18f-NLuc RNA (18f-NLuc/GAA) (*SI Appendix*, Fig. S1*G*). These results indicate that ZCCHC14 is not required for initial viral protein synthesis. Hepatovirus translation initiates in a cap-independent manner under control of an unusual internal ribosome entry site (IRES) that requires the cap-binding eukaryotic translation initiation factor 4E (eIF-4E) (23, 24). Since a previous study suggested that ZCCHC14 may be required for translation initiated by the HAV IRES (16), we assessed the impact of ZCCHC14 KO in cells transfected with plasmid DNA from which green fluorescent protein (GFP) can be synthesized only by HAV IRES-mediated internal initiation of translation on a back-spliced, circular RNA (circRNA) transcript (25). Notably, there was no decrease in GFP synthesized from the circRNA in ZCCHC14-KO cells (Fig. 1*F*), indicating no reduction in IRES activity. Similarly, IRES activity was little changed when assessed with bicistronic reporter constructs (*SI Appendix*, Fig. S1*H*), and polysome analysis demonstrated normal HAV RNA loading onto 80S ribosomes and translating polysomes in ZCCHC14-KO cells (Fig. 1*G* and *SI Appendix*, Fig. S1*I*). Together with the absence of any reduction in early viral protein synthesis in ZCCHC14-KO cells (Fig. 1*E*), these data show that ZCCHC14 is not required for HAV IRES-directed translation, as previously proposed (16).

Although mechanistic details are lacking, the noncanonical TENT4A/B poly(A) polymerases (also known as PAPD5/7) have also been found to be essential for HAV replication (16). Single-guide RNAs (sgRNAs) targeting TENT4 genes were not enriched in our CRISPR screen for HAV host factors (15) (*SI Appendix*, Fig. S1*B*), but targeted CRISPR deletion of TENT4B inhibited HAV replication 10-fold, whereas dual TENT4A/B deletion reduced it 20-fold (Fig. 1*H*). Similar results were obtained by siRNA-mediated TENT4A/B depletion (*SI Appendix*, Fig. S2*A*), with the magnitude of depletion by individual siRNAs correlating well with reductions in HAV replication (*SI Appendix*, Fig. S2 *B* and *C*). Consistent with this, the S-isomer (but not the R-isomer) of RG7834, a small-molecule dihydroquinolizinone inhibitor of TENT4A/B (18, 26), potently suppressed HAV replication without evidence of cytotoxicity in Huh-7.5 cells (half-maximal inhibitory concentration [IC_{50}] = 6.11 nM) (Fig. 1*I* and *SI Appendix*, Fig. S3 *A* and *B*). RG7834 similarly blocked amplification of the subgenomic HAV RNA replicon (*SI Appendix*, Fig. S3*C*). HAV replication was also inhibited by BCH001, a chemically unrelated TENT4B inhibitor (27) (IC_{50} = 9.14 μM) (*SI Appendix*, Fig. S3*D*). Collectively, these results point to a crucial role for TENT4A/B in HAV replication. In sharp contrast, chemical inhibition of TENT4A/B with RG7834 had no effect on the replication of poliovirus or human parechovirus 1, which are other picornaviruses (*SI Appendix*, Fig. S3 *E* and *F*).

RG7834 treatment did not reduce NLuc expression 2 to 6 h after 18f-NLuc infection (Fig. 1*J* and *SI Appendix*, Fig. S3*G*), before the onset of viral RNA synthesis, nor did it inhibit the translation of circRNA directed by the HAV IRES (*SI Appendix*, Fig. S3*H*). We also found that RG7834 had no effect on the stability of electroporated genome-length HAV RNA (*SI Appendix*, Fig. S3*I*). The impact of RG7834 on NLuc expression from transfected 18f-NLuc RNA mirrored that of the picornaviral replication inhibitor guanidine (28), and was strikingly different from the general translation inhibitor cycloheximide (*SI Appendix*, Fig. S3*J*). Taken collectively, these data suggest that TENT4 inhibition blocks viral RNA synthesis, not translation of the viral genome. Consistent with these results, RG7834 significantly reduced the incorporation of 5-ethynyl uridine (5EU) into nascent HAV RNA in an assay for viral RNA synthesis, while having no effect on nascent actin mRNA synthesis over a 24-h treatment window (Fig. 1*K*).

Cytoplasmic mRNA tailing by TENT4A/B posttranscriptionally regulates the stability of certain cellular mRNAs and, as a result, gene expression (29–31). The terminal nucleotidyltransferase activities of TENT4A/B are relatively promiscuous, and guanosine or uridine residues incorporated into 3′ poly(A) impede carbon catabolite repression 4-negative on TATA-less (CCR4-NOT) complex-mediated deadenylation, stabilizing mRNA (30). Hepatitis B virus (HBV) and human cytomegalovirus (hCMV) exploit this mechanism to stabilize key viral RNAs to promote viral replication (17). ZCCHC14 binds short stem-loop structures in these RNAs with pentaloop sequences conforming to the Smaug recognition motif to which it recruits TENT4 (17, 32). RG7834 blocks the nucleotidyltransferase activity of these noncanonical polymerases, resulting in shorter poly(A) tails and reduced viral RNA stability, thereby suppressing HBV replication (18, 26, 33, 34). Consistent with these published results, we found ZCCHC14 coimmunoprecipitated with FLAG-tagged TENT4A/B expressed in 293T cells (*SI Appendix*, Fig. S3*K*). We also found high concentrations of RG7834 disrupted the coimmunoprecipitation of ZCCHC14 with TENT4A/B (*SI Appendix*, Fig. S3*K*). Unlike the 3′ poly(A) tail of HBV RNAs, the 3′ poly(A) tail of HAV RNA is intrinsic to its positive-sense RNA genome (Fig. 1*A*) and transcribed by the viral RNA-dependent RNA polymerase, $3D^{pol}$ (4). This suggests that the role of TENT4 in HAV replication is likely to be fundamentally different from its role in HBV replication. Consistent with this, RG7834 treatment did not alter the length of the HAV 3′ poly(A) tail (Fig. 1 *L* and *M*).

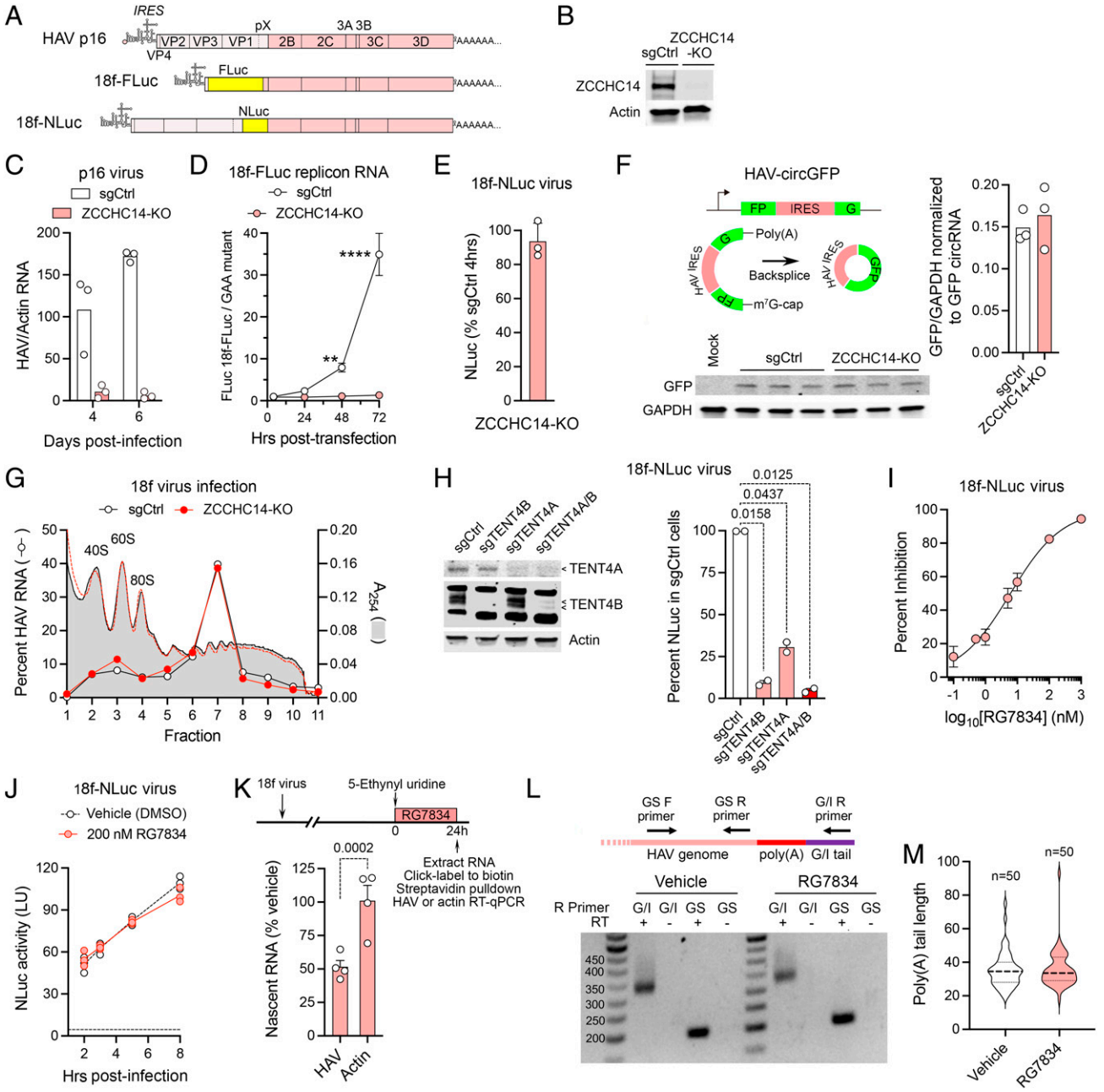

Fig. 1. Hepatovirus RNA synthesis requires ZCCHC14 and TENT4A/B. (*A*) Organization of the HAV genome, subgenomic 18f-FLuc replicon, and 18f-NLuc reporter virus genome. (*B*) ZCCHC14 immunoblot of ZCCHC14-KO and control (sgCtrl) cells. (*C*) HAV RNA abundance in ZCCHC14-KO and sgCtrl cells 4 and 6 d postinfection (p.i.) with p16 virus. (*D*) Firefly luciferase (FLuc) expressed by ZCCHC14-KO and sgCtrl cells transfected with HAV-FLuc replicon RNA. Data are representative of 2 independent experiments, each with 3 technical replicates, and are shown as means ± SDs relative to FLuc expressed by the replication-incompetent HAV-FLuc/GAA RNA mutant. $^{**}P = 0.0012$, $^{****}P < 0.0001$ by 2-way ANOVA with Šídák's multiple comparisons test. (*E*) NLuc expressed by ZCCHC14-KO cells relative to sgCtrl cells 4 h p.i. ± SD with 18f-NLuc virus. Mean NLuc expression was 12.7-fold above background. $n = 3$ independent experiments, each with 3 technical replicates. (*F*, *Left*) circRNA HAV IRES reporter assay showing GFP synthesized from back-spliced RNA in ZCCHC14-KO and sgCtrl cells. (*Right*) Quantitation of GFP normalized to glyceraldehyde 3-phosphate dehydrogenase (GAPDH) protein in immunoblots and back-spliced RNA measured by specific RT-PCR assay. Data shown are technical replicates from 1 of 2 independent experiments with similar results. (*G*) Polysome analysis of ZCCHC14-KO and sgCtrl cells 6 h after 18f virus infection, showing distribution of HAV RNA among ribosomes and polysomes separated by gradient centrifugation. Actin mRNA distribution is shown in *SI Appendix*, Fig. S1 *I*. (*H*, *Left*) Immunoblots of TENT4 proteins in Huh-7.5 cells transduced with lentiviruses expressing guide RNAs targeting TENT4A, TENT4B, or both TENT4A and 4B (TENT4A/B) or a scrambled sgRNA (sgCtrl). (*Right*) NLuc expressed 48 h after infection of CRISPR-edited TENT4 knockout Huh-7.5 cells shown in the blots on the left. Data shown are mean percent NLuc relative to infected sgCtrl cells from 2 experiments, each with 3 technical replicates. *P* values by 1-way ANOVA with Geisser-Greenhouse correction and Dunnett's multiple comparison test. (*I*) NLuc expressed by 18f-NLuc virus in Huh-7.5 cells 48 h p.i. with increasing concentrations of RG7834. Data shown are technical replicates from 1 of 2 experiments with similar results. (*J*) NLuc expressed by 18f-NLuc virus in Huh-7.5 cells 2–8 h p.i. in the presence or absence of 200 nM RG7834. Data from 1 of 2 independent experiments with similar results, each with 3 technical replicates. (*K*) Nascent HAV RNA synthesis assay. 18f virus-infected cells were metabolically labeled with 5-ethynyl uridine (5EU) for 24 h following the addition of RG7834 (200 nM) or DMSO. RNA was isolated, click-labeled with biotin, and captured on streptavidin beads for quantitation of nascent HAV and actin mRNA. Nascent RNA in DMSO-treated cells was arbitrarily set to 100. Results shown are means ± SEMs from 3 independent experiments, 1 with 2 technical replicates. (*L*) HAV poly(A) tail length assay. 18f virus-infected Huh-7.5 cells were treated with RG7834 (200 nM) or vehicle (DMSO) for 3 d. Total RNAs were extracted, guanosine and inosine (G/I) tailed, reverse transcribed (RT) and PCR amplified using genome-specific (GS) forward (F) and either GS or G/I-specific reverse (R) primers. PCR products were analyzed by agarose gel electrophoresis. Results shown are representative of two independent experiments. (*M*) HAV poly(A) tail length determined by sequencing 50 individual cDNA clones generated from RG7834 and vehicle-treated samples. Graph depicts median and quartile lengths; mean was 35.80 ± 11.2 SD nt for RG7834 versus 35.48 ± 10.71 SD for vehicle.

CLIP-Seq Reveals ZCCHC14 Binds Stem-Loop Vb in the HAV 5′ UTR. Coimmunoprecipitation experiments indicated that ZCCHC14 associates with HAV RNA in infected cells (Fig. 2*A*). UV crosslinking followed by immunoprecipitation and high-throughput sequencing of isolated crosslinked RNA (CLIP-seq) revealed abundant RNA crosslinked to FLAG-tagged ZCCHC14 expressed in infected cells (*SI Appendix*, Fig. S4*A*). Sequences within the 3′ end of the 5′ UTR (domain V) (35) were highly enriched over size-matched input RNA (Fig. 2 *B* and *C*). A total of 4,543 cellular RNA sequences were also significantly enriched in the crosslinked RNA, with most mapping to the 3′ UTR of mRNAs (*SI Appendix*, Fig. S4*B* and Table S1). Pull-down experiments using biotinylated RNA probes confirmed that ZCCHC14 and TENT4A associate with the 5′ UTR, whereas a 3′ UTR probe bound neither ZCCHC14 nor TENT4A (Fig. 2*D*).

Close inspection of the CLIP-seq results revealed discreet peaks mapping to previously established RNA structure within the HAV IRES, including in particular the 3′ half of domain V, which includes two small stem-loops: Vb and Vc (35) (Fig. 2 *B* and *C* and *SI Appendix*, S4*C*). Vb was of particular interest, as its structure has been defined by X-ray crystallography (36) and its pentaloop sequence (CUGGA) conforms to the Smaug recognition element that binds ZCCHC14 (17, 32). A biotinylated RNA probe representing the Vb sequence bound both ZCCHC14 and TENT4A proteins, confirming Vb binds ZCCHC14 (Fig. 2*E*). Binding was largely abolished when the loop sequence was mutated (Fig. 2*E*). Importantly, the Vb probe failed to pull down TENT4A in lysates of ZCCHC14-KO cells, or after the addition of RG7834 (Fig. 2*E*). These results show that TENT4A is recruited to ZCCHC14 bound to stem-loop Vb, and they are consistent with RG7834 disrupting the ZCCHC14-TENT4A/B association, as described above (*SI Appendix*, Fig. S3*K*). We further assessed the linkage between ZCCHC14 and TENT4A/B by determining whether TENT4A/B inhibition and ZCCHC14 depletion have additive inhibitory effects on HAV replication. ZCCHC14 depletion alone reduced reporter virus replication by 98.2% ± 0.36% SD, whereas RG7834 treatment caused a 91.1% ± 1.6% SD reduction in ZCCHC14-replete cells (*SI Appendix*, Fig. S3*L*). By contrast, RG7834 reduced replication only 46.6% ± 11% SD in ZCCHC14-KO cells ($P = 0.0019$ by t test), indicating that the effects of RG7834 treatment and ZCCHC14 depletion are not strictly additive and likely affect the same step in viral replication.

Probes representing RNA sequence upstream of domain V or full-length 5′ UTR probes with mutated or deleted Vb loop sequence bound less ZCCHC14 and TENT4A protein than the Vb-wt probe (Fig. 2*F*). Although stem-loop Vb is positioned within the IRES, our previous studies show that it is not required for cap-independent HAV translation in reticulocyte lysates (35, 37). Consistent with this, deleting Vb or mutating its pentaloop sequence had no effect on translation of the circRNA IRES reporter (*SI Appendix*, Fig. S4*D*), but reduced the replication of the 18f-NLuc reporter virus by 75 to 80% (Fig. 2 *G* and *H*). The residual replication exhibited by the Vb mutants was ablated by knocking out ZCCHC14 (Fig. 2 *I*). Thus, while stem-loop Vb is the major determinant of ZCCHC14 binding to the 5′ UTR, some binding occurs outside its boundaries. This conclusion is consistent with the results of the CLIP-seq experiments, which suggest a minor ZCCHC14 interaction site near nucleotide 600, at the base of domain V (Fig. 2*B*).

RG7834 Ablates HAV Replication and Reverses Liver Inflammation in *Ifnar1*$^{-/-}$ Mice. To assess the therapeutic potential of RG7834, we administered the drug orally to *Ifnar1*$^{-/-}$ mice with acute HAV infection. These mice lack type I interferon receptors and are highly permissive for HAV, with infection recapitulating the cardinal features of hepatitis A in humans, including hepatocellular apoptosis, intrahepatic inflammatory cell infiltrates, and elevated serum alanine aminotransferase (ALT) activities (12). RG7834 (10 mg/kg b.i.d.) was given by gavage 6 d after intravenous (i.v.) challenge with 2×10^6 genome equivalents (GEs) of HAV, when serum ALT was ∼10-fold above normal (Fig. 3*A*). ALT levels fell dramatically in the treated animals, reaching normal by day 12 p.i., whereas levels continued to climb through day 8 in sham-treated controls (Fig. 3 *A*, *Top*). RG7834 treatment also reduced fecal HAV shedding (Fig. 3 *A*, *Bottom*). At necropsy, 12 d p.i., RG7834-treated mice had less viral RNA in the liver (Fig. 3 *B*) and normal liver histology (Fig. 3 *C* and *D*). In sharp contrast, the sham-treated animals had extensive intrahepatic inflammation and numerous apoptotic hepatocytes staining for cleaved caspase 3 (Fig. 3 *C–E* and *SI Appendix*, Fig. S5 *A* and *B*). Intrahepatic interferon-β (*Ifnb*) and proinflammatory *Ccl5*, *Cxcl10*, and *Ccl2* chemokine transcripts were markedly reduced in treated animals (Fig. 3*E*), reflecting less virus activation of innate immune response pathways. ALT levels rebounded off treatment, although they remained lower in mice that had received RG7834 than in the vehicle-treated cohort 7 d off treatment (Fig. 3*A*). At this point in time (19 d p.i.), ring-like collections of inflammatory cells were evident in liver from treated mice (Fig. 3*G* and *SI Appendix*, Fig. S5*A*). These annular infiltrates comprised $CD3^+$ T cells, $B220^+$ B lymphocytes, and $CD68^+$ macrophages, in close proximity to cells containing HAV RNA (*SI Appendix*, Fig. S5 *C–E*). HAV was not detected in feces after stopping RG7834 treatment (Fig. 3*A*), but increases in intrahepatic *Ifnb* and chemokine transcripts were consistent with virologic relapse (*SI Appendix*, Fig. S5*F*). Treatment did not impair viral neutralizing antibody responses (Fig. 3*H*), nor virus-specific $CD8^+$ T cell responses in animals studied 32 d p.i. (Fig. 3 *I* and *J*).

To better assess the potential for relapse following RG7834 treatment, we infected *Ifnar1*$^{-/-}$ mice with a 10-fold greater viral inoculum (2×10^7 GE), administering RG7834 beginning 4 to 5 d p.i. Serum ALT levels and fecal HAV RNA shedding rapidly diminished in treated animals (Fig. 3*K* and *SI Appendix*, Fig. S6 *A* and *B*). Intrahepatic HAV RNA was reduced threefold after 72 h of treatment (*SI Appendix*, Fig. S6*C*). Apoptotic hepatocytes were scarce in animals receiving RG7834, but frequent and associated with substantial inflammation in sham-treated controls (*SI Appendix*, Fig. S6 *D–F*). Serum ALT similarly declined in mice treated with a lower dose of RG7834 (2.5 mg/kg b.i.d.), reaching baseline levels after 6 d when treatment was stopped (Fig. 3*K*). Fecal virus shedding was also reduced, yet still detected at the end of treatment (Fig. 3*L*). However, within 1 week of discontinuing RG7834, ALT levels had rebounded in all of the treated animals (Fig. 3*K*), and at necropsy, intrahepatic viral RNA levels and inflammatory changes in the liver were comparable to sham-treated animals (*SI Appendix*, Fig. S6 *G–J*). Taken collectively, these data show that RG7834 has strong antiviral activity in animals with established infection and can interrupt HAV pathogenesis in vivo. However, extended treatment may be required to prevent virologic relapse in immunocompromised animals such as *Ifnar1*$^{-/-}$ mice. The ability of RG7834 to ameliorate viral-induced liver injury is HAV specific, as RG7834 treatment neither inhibited virus replication nor lowered serum ALT elevations in mice infected with lymphocytic choriomeningitis virus (LCMV-clone13) (*SI Appendix*, Fig. S7).

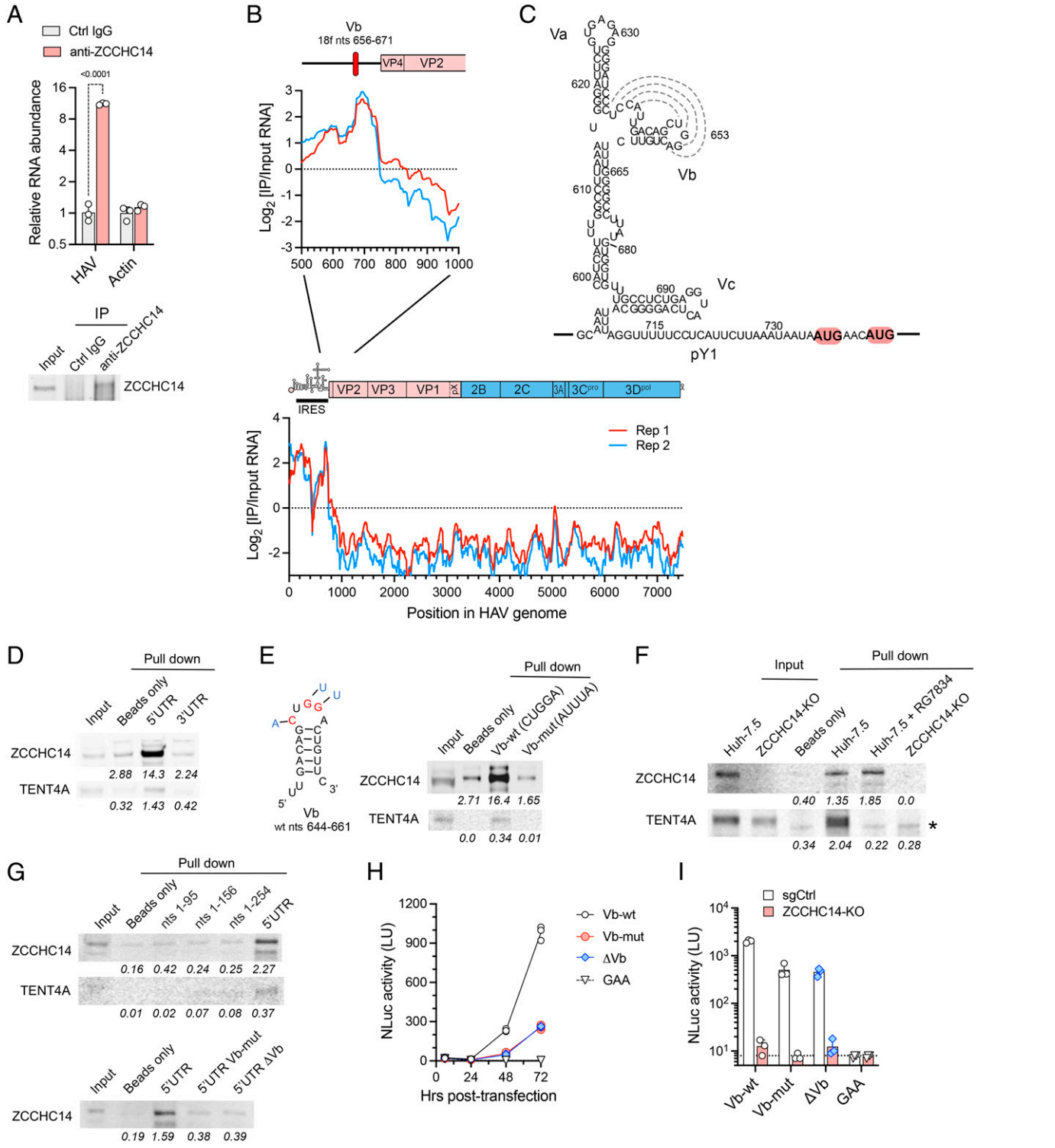

Fig. 2. ZCCHC14 binds stem-loop Vb and recruits TENT4A to the HAV 5′ UTR. (*A*) Coimmunoprecipitation of HAV RNA with ZCCHC14 from lysates of 18f-infected Huh-7.5 cells. HAV genomic RNA and actin mRNA were quantified by qRT-PCR in immunoprecipitates and normalized to spiked-in GLuc RNA with RNA abundance in isotype control (Ctrl) precipitates arbitrarily set to 1.0. $n = 3$ independent experiments. ZCCHC14 immunoblot shown below. (*B*) FLAG-ZCCHC14 CLIP-seq result in 18f-infected 293T cells showing coverage of HAV-specific reads in 2 independent assays (blue and red tracks). Data are shown as $\log_2$ of the ratio of reads recovered from the immunoprecipitate to input RNA, aligned to the HAV 18f genome. An expanded view of reads mapping to nucleotides 500–1,000 is shown at the top. (*C*) Secondary structure of domain V (nucleotides 596–709) of the wild-type HAV 5′ UTR (35), showing stem-loops Va, Vb, and Vc. Dashed lines indicate potential pseudoknot structure (35). pY2, pyrimidine-rich tract 2. (*D*) RNA pull down using full-length synthetic 3′ biotinylated HAV 5′ UTR and 5′ biotinylated 3′ UTR baits. RNA baits were incubated with Huh-7.5 cell lysate, then affinity purified on streptavidin beads. Copurified ZCCHC14 and TENT4A proteins were detected by immunoblotting. Relative fluorescence intensities within each blot are noted in italicized text. (*E*) ZCCHC14 and TENT4A pulldown with a 3′ biotinylated synthetic probe representing stem-loop Vb (nucleotides 644–661) and Vb-mut; nucleotide substitutions in Vb-mut (blue) ablate the CNGGN loop. (*F*) ZCCHC14 and TENT4A proteins pulled down with the Vb-wt probe from lysates of Huh-7.5 cells, in the presence and absence of 500 nM RG7834, and ZCCHC14-KO cells. *Nonspecific band. (*G*) RNA pull-down assays using (*Top*) RNA probes representing sequences upstream of domain V (nucleotides 1–95, 1–156, or 1–254) or (*Bottom*) full-length 5′ UTR sequence with either Vb loop substitutions (Vb-mut, see panel *E*) or complete deletion of Vb (ΔVb). (*H*) NLuc expressed by Huh-7.5 cells transfected with 18f-NLuc virus RNA with wild-type (Vb-wt), mutant (Vb-mut) or deleted (ΔVb) stem-loop Vb. Replication-incompetent RNA (Δ3D) was included as a control. (*I*) NLuc expressed 72 h after transfection of the 18f-NLuc Vb reporter virus mutants in sgCtrl versus ZCCHC14-KO cells. GAA, replication-incompetent virus mutant.

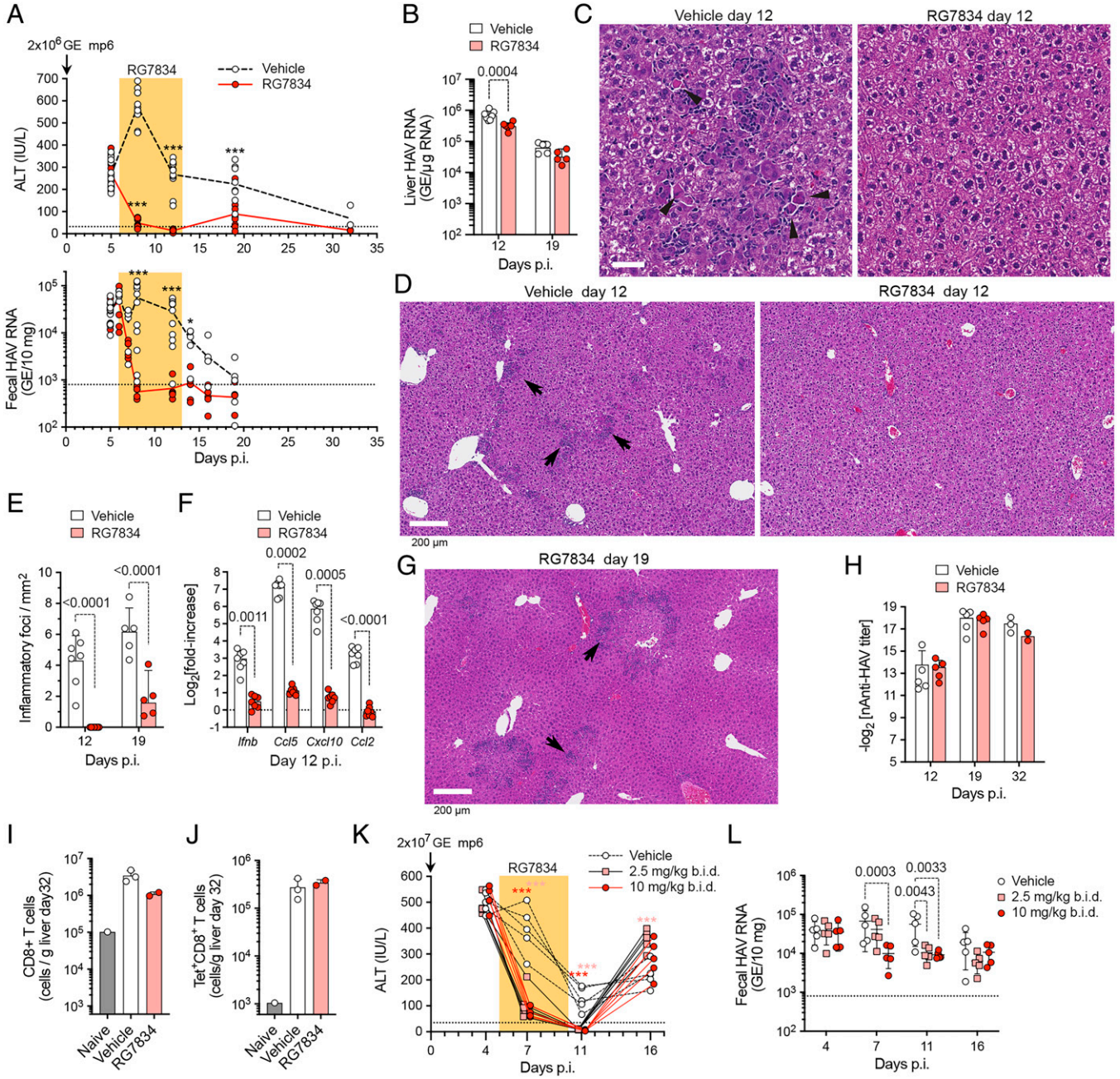

Fig. 3. RG7834 treatment of acute hepatitis A in *Ifnar1*$^{-/-}$ mice. (*A*) (*Top*) Serum ALT activities (***$P < 0.001$) and (*Bottom*) fecal HAV RNA quantified by qRT-PCR in mice treated with RG7834 10 mg/kg per os (p.o.) b.i.d. or vehicle only between days 6 and 12 p.i. with 2×10^6 genome equivalents (GEs) of wild-type HM175-mp6 virus. $n = 12$–15 mice in each group between days 6–16, 8 on day 19, and 2–3 at day 33. *$P = 0.016$ by t test; ***$P \leq 0.001$. (*B*) Geometric mean HAV RNA copies per microgram total RNA, ±95% confidence interval (CI), in liver tissue from mice in panel *A* on days 12 and 19 p.i. *$P = 0.040$ by Mann-Whitney test. (*C* and *D*) High (*C*) and low (*B*) magnification views of hematoxylin and eosin (H & E)–stained liver sections from mice in panel *A*. Tissues were collected on 12 (end of therapy) and 19 d p.i. Apoptotic hepatocytes are surrounded by inflammatory infiltrates (arrows). (*E*) Numbers of inflammatory foci per square millimeter in H & E-stained sections of livers. (*F*) Interferon-β and proinflammatory chemokine transcript levels determined by RT-PCR in livers harvested from mice in panel *A* on day 12, relative to levels expressed in naïve mice. *P* values by t test with Welch correction and Holm-Šídák test for multiple comparisons. (*G*) H & E-stained liver from an RG7834-treated animal in panel *A* on day 19. (*H*) Serum HAV-neutralizing antibody titers in HAV-infected mice in panel *A*. (*I*) Total CD8$^+$ T cells and (*J*) HAV-specific tetramer-positive CD8$^+$ T cells enumerated by flow cytometry in liver tissues 32 d p.i. in mice treated with RG7834 as in panel *A*. (*K*) Serum ALT activities in mice infected with high-titer HAV (2×10^7 GE) and treated with RG7834, 10 mg/kg or 2.5 mg/kg b.i.d., or vehicle only ($n = 5$ in each group) between days 5 and 9 p.i. ***$P < 0.0001$ versus sham treated by 2-way ANOVA with Dunnett's multiple comparison test. (*L*) Fecal HAV shedding by mice shown in panel *H*. Statistical testing as in panel *H*. Dashed horizontal lines indicate limits of detection. Error bars represent SDs in all panels, unless noted otherwise.

Chemoprevention of Hepatitis A in *Ifnar1*$^{-/-}$ Mice. Consistent with its strong antiviral activity, a brief course of RG7834 therapy given as postexposure prophylaxis completely prevented hepatitis A in *Ifnar1*$^{-/-}$ mice (Fig. 4*A*). ALT levels remained normal and there was no detectable fecal virus shedding in mice treated for 5 d with 10 mg/kg b.i.d. beginning immediately after inoculation with a large inoculum (2×10^7 GE virus) (Fig. 4 *B* and *C*). Only low levels of intrahepatic viral RNA, near the limit of detection, were identified at necropsy 16 d later (Fig. 4*D*). Remarkably, there was no detectable serum neutralizing antibody in treated mice (titer <1:80), whereas the geometric mean titer (GMT) of neutralizing

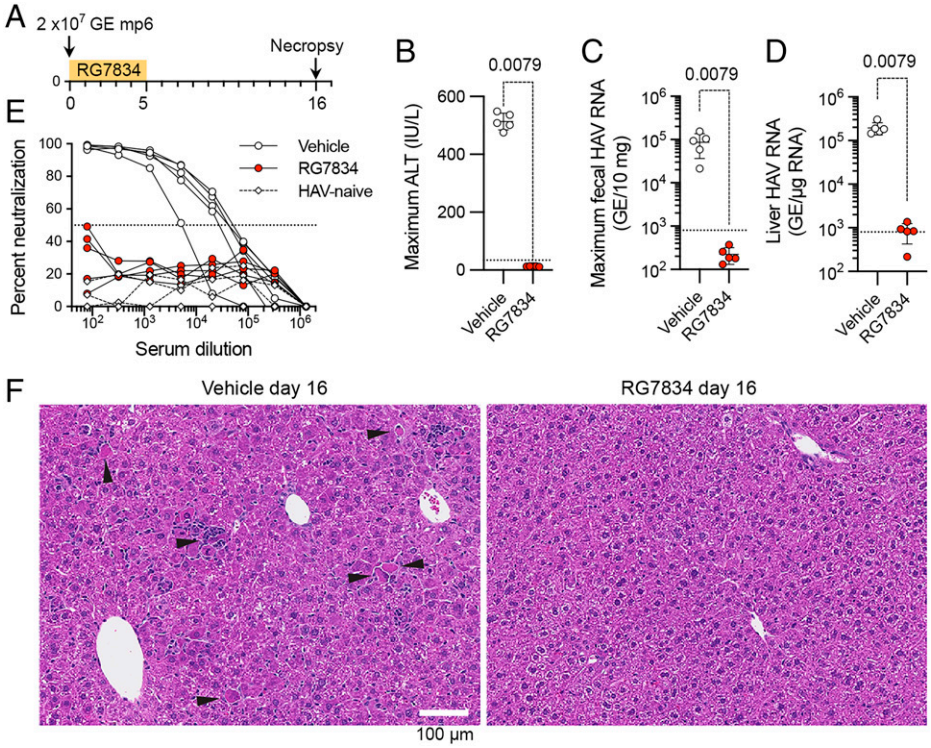

Fig. 4. Chemoprevention of hepatitis A in *Ifnar1*$^{-/-}$ mice. (*A*) Experimental plan, showing groups of mice (n = 5 each) given postexposure prophylaxis with RG7834 10 mg/kg p.o. b.i.d. or sham treated with vehicle only for 5 d commencing immediately after i.v. challenge with 2×10^7 GE HAV. Mice were followed twice weekly for serum ALT elevation and fecal virus shedding until necropsy on day 19 p.i. (*B*) Maximum ALT elevation and (*C*) maximum fecal HAV RNA shedding in mice between virus challenge and necropsy at day 19 p.i. (*D*) Intrahepatic HAV RNA at necropsy on day 19 p.i. (*E*) Neutralization of HM175/18f-NLuc virus by fourfold dilutions of serum collected on day 19 p.i. from mice receiving RG7834 or vehicle only. Neutralization is shown as inhibition of NLuc expressed by Huh-7.5 cells 72 h p.i. with serum-virus mixtures, relative to sera from 4 HAV-naïve mice (mean 6.6×10^2 light units). (*F*) Representative H & E-stained liver sections from mice receiving postexposure prophylaxis with RG7834 or vehicle only as in panel *A*. Arrows indicate apoptotic hepatocytes. Statistical testing of ALT and HAV RNA levels by Mann-Whitney test. Dashed horizontal lines indicate limits of detection. Error bars represent SDs.

antibodies 16 d p.i. in sham-treated mice was 1:27,014 (Fig. 4*E*). The histologic appearance of the liver was normal in animals given RG7834, whereas there were numerous inflammatory foci and apoptotic hepatocytes in sham-treated mice (Fig. 4*F*). Thus, RG7834 prevented HAV replication when administered immediately after virus challenge.

Discussion

The noncanonical TENT4 poly(A) polymerases are known to remodel the 3′ poly(A) tails of some cellular mRNAs resulting in random 3′ RNA guanylation that interferes with deadenylation by the CCR4-NOT complex and stabilizes the mRNA (30, 38). HBV usurps this activity of the TENT4 polymerases, which similarly lengthen and guanylate the 3′ poly(A) tails of HBV mRNAs, enhancing their stability and promoting replication of the virus. The dihydroquinolizinone RG7834 inhibits this stabilizing activity of TENT4, leading to its initial clinical development as a therapy for chronic hepatitis B (34, 39). However, in contrast to HBV mRNA, RG7834 has no effect on the length of the 3′ poly(A) tail of HAV (Fig. 1*M*), indicating that it has an alternative antiviral mechanism of action against HAV. Kulsuptrakul et al. suggested that ZCCHC14 and TENT4A/B are required for cap-independent translation initiated by the HAV IRES (16). However, we found that the translation-initiating activity of the HAV IRES was not diminished by ZCCHC14 KO (Fig. 1 *F* and *G*), and that viral protein synthesis was not impaired by RG7834 treatment 2 to 6 h after infection, before viral RNA amplification (Fig. 1*J*). By contrast, metabolic labeling experiments indicated that RG7834 significantly reduces viral RNA synthesis (Fig. 1*K*). Thus, the ZCCHC14-TENT4 complex contributes to a later step in the replication cycle, following viral protein translation.

Why only certain mRNAs are targeted for 3′ modification by the TENT4 polymerases is unknown. Specific recognition motifs have been proposed to exist within these mRNAs, but they have never been identified (30). Although we did not find TENT4 in pull-down experiments using the 3′ UTR as bait (Fig. 2*D*), recognition of the 3′ end of the genomic RNA by TENT4A/B bound to ZCCHC14 at the 5′ UTR could play an important role in replication by providing a protein bridge functionally circularizing the viral RNA (Fig. 5). RG7834 could then interrupt this interaction by binding TENT4 (26). Although speculative, this model is consistent with well-documented requirements for protein–protein or RNA–RNA interactions bridging the 5′ and 3′ ends of the genome in replication of other positive-strand RNA viruses, including some picornaviruses (40–43). Such a mechanism would not necessarily require the terminal nucleotide transferase activities of TENT4A/B and, indeed, whether the catalytic activity of TENT4 is required for HAV replication remains to be determined. Despite strong pharmacologic (RG7834) and genetic evidence for an on-target, TENT4-specific effect of RNAi TENT4A/B depletion (*SI Appendix*, Fig. S2), we were unable to rescue replication by ectopically expressing each of the known TENT4B transcripts.

The HAV RNA-dependent RNA polymerase 3D^{pol} remains poorly characterized and has never been expressed in active form. It is intriguing to consider the possibility that TENT4 somehow contributes to either genome transcription or uridylation

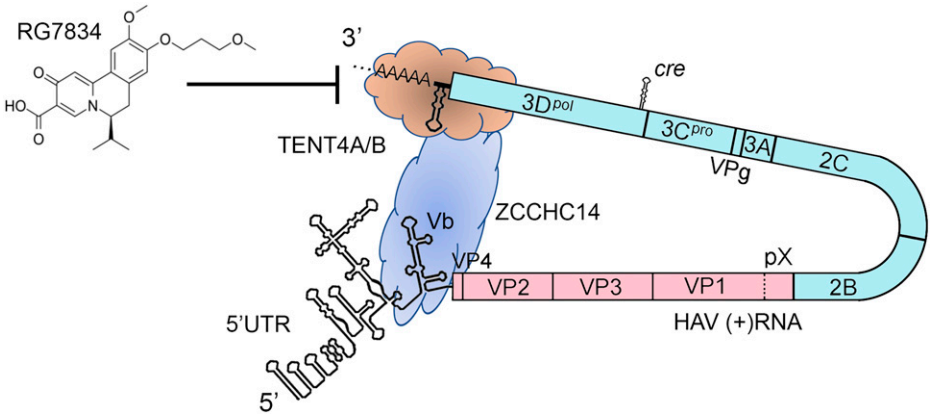

Fig. 5. Model explaining RG7834 inhibition of hepatovirus RNA synthesis. TENT4A/B is recruited to ZCCHC14 bound to stem-loop Vb within the 5′ UTR, and recognizes the 3′ end of the polyadenylated HAV genome, providing a protein bridge that functionally circularizes the genome, thereby promoting viral RNA synthesis. RG7834 binds to and interrupts the interaction of TENT4A/B with ZCCHC14, disrupting circularization of the genome and impeding replication.

of the VPg primer for RNA synthesis, a process that in enteroviruses is dependent in part on the $3D^{pol}$ polymerase (44). However, the location of the stem-loop to which ZCCHC14-TENT4 is recruited (nucleotides 644 to 660) is far upstream of the *cis*-acting replication element (*cre*, nucleotides 5,948 to 6,057) that templates the uridylation reaction (45) (Fig. 5), making this unlikely.

Although the mechanism by which TENT4 contributes to HAV replication requires further study, its role as an essential host factor provides an unexpected opportunity for both antiviral therapy and chemoprevention of hepatitis A. Historically, hepatitis A has been well controlled by immunization in the United States, but in recent years, we have seen unprecedented numbers of HAV infections with numerous hospitalizations and fatalities (1–3). Our data show that oral delivery of RG7834, a dihydroquinolizinone TENT4 inhibitor, blocks HAV replication and profoundly interrupts pathogenesis in a murine model of hepatitis A (Figs. 3 and 4). The safety of RG7834 was evaluated in a phase 1 ascending-dose clinical trial involving 49 participants without reported adverse effects (ClinicalTrials.gov NCT02604355). However, the compound has not progressed further due to toxicity concerns identified in long-term animal exposure studies. Hepatoselective dihydroquinolizinones have been developed that may be less toxic (46). We evaluated the antiviral activity of one such compound (DHQ-E-OH) and found that it inhibited 18f-NLuc reporter virus replication in cell culture with an IC_{50} of 278 nM. Experiments in *Ifnar1*$^{-/-}$ mice suggest that short-term pharmacologic intervention with RG7834 or potentially less-toxic hepatoselective compounds may have substantial clinical benefit and could be lifesaving in severe hepatitis A. Both passive and active immunization regimens are used widely for postexposure prophylaxis of hepatitis A, but neither provide a high level of protection when instituted more than 2 wk after exposure (47). An effective antiviral could significantly extend the opportunities for intervening and preventing disease in outbreak settings.

Materials and Methods

Cells. Polyclonal Huh-7.5 ZCCHC14-KO cells, TENT4A-KO and TENT4B-KO cells, and doubly knocked-out TENT4A/B-KO cells were generated using precloned commercial lentivirus vectors. See *SI Appendix, Materials and Methods* for additional details.

Viruses. The cell-culture-adapted HAV variants HM175/p16 (p16) and HM175/18f (18f) and the 18f-NLuc reporter virus have been described previously (19–21). Mouse-passaged wild-type HM175 strain HAV was used at the sixth mouse passage level and prepared from homogenates of liver from infected *Mavs*$^{-/-}$ mice as described (12). See also *SI Appendix, Materials and Methods*.

Nascent RNA Synthesis Assay. Nascent RNA transcripts were quantified using the Click-iT Nascent RNA Capture Kit (C10365, Thermo Fisher Scientific) according to the manufacturer's protocol with some modifications. Huh-7.5 cells were infected with 18f virus for 5 d, then refed with media containing 0.5 mM 5EU and 200 mM RG7834 and incubated for an additional 24 h. Total RNAs were extracted using the RNeasy Mini Kit (Qiagen). Five micrograms total RNA and 0.5 mM biotin azide were used in a copper-catalyzed click reaction to conjugate biotin to 5EU-labeled RNA. Following precipitation, the RNA was dissolved in 50 μL RNase-free water. Biotin-conjugated 5EU-labeled RNA was isolated from 3 μg total RNA on streptavidin magnetic beads and used as a template for qRT-PCR (see above).

CLIP- and RNA-Seq. 293T cells were infected with 18f virus for 3 d, then transfected with FLAG-ZCCHC14 plasmid and harvested 2 d later. CLIP-seq was carried out as described previously (48), but with several modifications. UV cross-linking was carried out in a Stratagen UV Crosslinker using the "auto" setting. Cell lysis and RNase treatment were carried out as described (48). Immunoprecipitation was performed with anti-FLAG magnetic beads (M8823, Millipore). Cross-linked RNAs were ligated with 3′ IRDye800 labeled adapters (AGAUCGGAAGAGCGUCGUGAAAAAAAAA/3IRDye800/). Immunoprecipitated proteins and RNAs were examined by sodium dodecyl sulfate-polyacrylamide gel electrophoresis (SDS-PAGE). Cross-linked RNAs were purified, reversed transcribed, and libraries were generated as described (48). Libraries were sequenced on an Illumina Hiseq4000 sequencer by Genewiz with the paired-end 150-bp setting. Barcode sequences were trimmed from the sequencing reads and PCR duplicates were removed. Processed reads were aligned to the human hg19 genome and HAV HM175/18f virus sequence with STAR/2.7.3a. Peaks enriched for reads mapping to HAV RNA were analyzed with deeptools/3.2.0. Peaks enriched for reads mapping to cellular RNAs were identified with the CLIPper program as described (48), and annotated with HOMER version 4.11 (homer.ucsd.edu/homer/). Raw data have been deposited at the Gene Expression Omnibus (GEO) repository: GSE192599. See also *SI Appendix, Materials and Methods*.

Data Availability. High-throughput RNA-seq data generated in the CLIP-seq experiments have been deposited in GEO (GSE192599) (49). All other data generated or analyzed during this study are included in the article or supporting information.

ACKNOWLEDGMENTS. We thank Dr. Narry Kim (Seoul National University) for the gift of the TENT4 expression vectors, and Drs. Timothy Block and Yanming Du (Baruch S. Blumberg Institute) for providing the DHQ-E-OH compound. This

work was supported in part by grants from the National Institute of Allergy and Infectious Diseases of the US NIH (R01-AI131685 to S.M.L. and J.K.W.; R01-AI103083; R01-AI150095 to S.M.L.; R21-AI163606 to Y.L. and I.M.; and R01-AI143894 and R01-AI138337 to J.K.W.). The University of North Carolina (UNC) Pathology Services Core and UNC High-Throughput Sequencing Facility were supported in part by NCI Center Core Support Grant P30CA016086 to the Lineberger Comprehensive Cancer Center.

Author affiliations: [a]Lineberger Comprehensive Cancer Center, The University of North Carolina at Chapel Hill, Chapel Hill, NC 27599; [b]Department of Medicine, The University of North Carolina at Chapel Hill, Chapel Hill, NC 27599-7292; [c]Department of Genetics, The University of North Carolina at Chapel Hill, Chapel Hill, NC 27599; [d]Department of Microbiology & Immunology, The University of North Carolina at Chapel Hill, Chapel Hill, NC 27599; and [e]College of Veterinary Medicine, North Carolina State University, Raleigh, NC 27607

Author contributions: Y.L., I.M., J.K.W., and S.M.L. conceived study and designed specific experiments; Y.L. carried out CLIP-seq, RNA–protein interaction, and siRNA and CRISPR depletion studies; Y.L. and E.M.L. performed polysome profiling; I.M., L.S., T.T., and J.E.M. carried out experiments in mice; T.S. and H.K. carried out antiviral activity assays; T.S., A.H.-W., and K.L.M. contributed to plasmid construction; C.E.C. and N.M. supervised antiviral and polysome assays; D.R.M. was responsible for FISH assays; Y.L., I.M., J.K.W., and S.M.L. designed research; Y.L., I.M., T.S., L.S., E.M.L., H.K., T.S., A.H.-W., T.T., J.E.M., K.L.M., and D.R.M. performed research; J.M.C. reviewed histopathology; T.S., C.E.C., and N.M. contributed new reagents/analytic tools; Y.L., I.M., D.R.M., J.M.C., J.K.W., and S.M.L. analyzed data; J.K.W. and S.M.L. provided overall supervision and coordination; Y.L., I.M., J.K.W., and S.M.L. drafted the manuscript, which was reviewed and edited by all co-authors; and Y.L., I.M., J.K.W., and S.M.L. wrote the paper.

1. M. G. Hofmeister *et al.*, Hepatitis A person-to-person outbreaks: Epidemiology, morbidity burden, and factors associated with hospitalization-multiple states, 2016-2019. *J. Infect. Dis.* **223**, 426–434 (2021).
2. Centers for Disease Control and Prevention, Hepatitis Outbreaks. (2021). https://www.cdc.gov/hepatitis/outbreaks/2017March-HepatitisA.htm
3. M. G. Hofmeister *et al.*, Factors associated with hepatitis A mortality during person-to-person outbreaks: A matched case-control study-United States, 2016-2019. *Hepatology* **74**, 28–40 (2021).
4. S. M. Lemon, J. J. Ott, P. Van Damme, D. Shouval, Type A viral hepatitis: A summary and update on the molecular virology, epidemiology, pathogenesis and prevention. *J. Hepatol.* **68**, 167–184 (2017).
5. K. L. McKnight, S. M. Lemon, Hepatitis A virus genome organization and replication strategy. *Cold Spring Harb. Perspect. Med.* **8**, a033480 (2018).
6. D. B. Smith, P. Simmonds, Classification and genomic diversity of enterically transmitted hepatitis viruses. *Cold Spring Harb. Perspect. Med.* **8**, a031880 (2018).
7. R. E. Lanford *et al.*, Acute hepatitis A virus infection is associated with a limited type I interferon response and persistence of intrahepatic viral RNA. *Proc. Natl. Acad. Sci. U.S.A.* **108**, 11223–11228 (2011).
8. A. Hirai-Yuki, L. Hensley, J. K. Whitmire, S. M. Lemon, Biliary secretion of quasi-enveloped human hepatitis A virus. *MBio* **7**, e01998-e01916 (2016).
9. Z. Feng *et al.*, A pathogenic picornavirus acquires an envelope by hijacking cellular membranes. *Nature* **496**, 367–371 (2013).
10. K. L. McKnight *et al.*, Protein composition of the hepatitis A virus quasi-envelope. *Proc. Natl. Acad. Sci. U.S.A.* **114**, 6587–6592 (2017).
11. C. M. Walker, Z. Feng, S. M. Lemon, Reassessing immune control of hepatitis A virus. *Curr. Opin. Virol.* **11**, 7–13 (2015).
12. A. Hirai-Yuki *et al.*, MAVS-dependent host species range and pathogenicity of human hepatitis A virus. *Science* **353**, 1541–1545 (2016).
13. I. Misumi *et al.*, T cells protect against hepatitis A virus infection and limit infection-induced liver injury. *J. Hepatol.* **75**, 1323–1334 (2021).
14. J. Kim *et al.*, Innate-like cytotoxic function of bystander-activated CD8(+) T cells is associated with liver injury in acute hepatitis A. *Immunity* **48**, 161–173.e5 (2018).
15. A. Das *et al.*, Gangliosides are essential endosomal receptors for quasi-enveloped and naked hepatitis A virus. *Nat. Microbiol.* **5**, 1069–1078 (2020).
16. J. Kulsuptrakul, R. Wang, N. L. Meyers, M. Ott, A. S. Puschnik, A genome-wide CRISPR screen identifies UFMylation and TRAMP-like complexes as host factors required for hepatitis A virus infection. *Cell Rep.* **34**, 108859 (2021).
17. D. Kim *et al.*, Viral hijacking of the TENT4-ZCCHC14 complex protects viral RNAs via mixed tailing. *Nat. Struct. Mol. Biol.* **27**, 581–588 (2020).
18. L. Sun *et al.*, The dihydroquinolizinone compound RG7834 inhibits the polyadenylase function of PAPD5 and PAPD7 and accelerates the degradation of matured hepatitis B virus surface protein mRNA. *Antimicrob. Agents Chemother.* **65**, e00640-20 (2020).
19. R. W. Jansen, J. E. Newbold, S. M. Lemon, Complete nucleotide sequence of a cell culture-adapted variant of hepatitis A virus: Comparison with wild-type virus with restricted capacity for in vitro replication. *Virology* **163**, 299–307 (1988).
20. M. Yi, S. M. Lemon, Replication of subgenomic hepatitis A virus RNAs expressing firefly luciferase is enhanced by mutations associated with adaptation of virus to growth in cultured cells. *J. Virol.* **76**, 1171–1180 (2002).
21. D. Yamane *et al.*, Basal expression of interferon regulatory factor 1 drives intrinsic hepatocyte resistance to multiple RNA viruses. *Nat. Microbiol.* **4**, 1096–1104 (2019).
22. E. E. Rivera-Serrano, O. González-López, A. Das, S. M. Lemon, Cellular entry and uncoating of naked and quasi-enveloped human hepatoviruses. *eLife* **8**, e43983 (2019).
23. A. M. Borman, Y. M. Michel, K. M. Kean, Detailed analysis of the requirements of hepatitis A virus internal ribosome entry segment for the eukaryotic initiation factor complex eIF4F. *J. Virol.* **75**, 7864–7871 (2001).
24. I. K. Ali, L. McKendrick, S. J. Morley, R. J. Jackson, Activity of the hepatitis A virus IRES requires association between the cap-binding translation initiation factor (eIF4E) and eIF4G. *J. Virol.* **75**, 7854–7863 (2001).
25. R. M. Meganck *et al.*, Tissue-dependent expression and translation of circular RNAs with recombinant AAV vectors in vivo. *Mol. Ther. Nucleic Acids* **13**, 89–98 (2018).
26. H. Mueller *et al.*, PAPD5/7 are host factors that are required for hepatitis B virus RNA stabilization. *Hepatology* **69**, 1398–1411 (2019).
27. N. Nagpal *et al.*, Small-molecule PAPD5 inhibitors restore telomerase activity in patient stem cells. *Cell Stem Cell* **26**, 896–909.e8 (2020).
28. E. A. Tolskaya *et al.*, Genetic studies on the poliovirus 2C protein, an NTPase. A plausible mechanism of guanidine effect on the 2C function and evidence for the importance of 2C oligomerization. *J. Mol. Biol.* **236**, 1310–1323 (1994).
29. J. Shin, K. Y. Paek, M. Ivshina, E. E. Stackpole, J. D. Richter, Essential role for non-canonical poly(A) polymerase GLD4 in cytoplasmic polyadenylation and carbohydrate metabolism. *Nucleic Acids Res.* **45**, 6793–6804 (2017).
30. J. Lim *et al.*, Mixed tailing by TENT4A and TENT4B shields mRNA from rapid deadenylation. *Science* **361**, 701–704 (2018).
31. S. Yu, V. N. Kim, A tale of non-canonical tails: Gene regulation by post-transcriptional RNA tailing. *Nat. Rev. Mol. Cell Biol.* **21**, 542–556 (2020).
32. T. Aviv *et al.*, The RNA-binding SAM domain of Smaug defines a new family of post-transcriptional regulators. *Nat. Struct. Biol.* **10**, 614–621 (2003).
33. A. Hyrina *et al.*, A genome-wide CRISPR screen identifies ZCCHC14 as a host factor required for hepatitis B surface antigen production. *Cell Rep.* **29**, 2970–2978.e6 (2019).
34. H. Mueller *et al.*, A novel orally available small molecule that inhibits hepatitis B virus expression. *J. Hepatol.* **68**, 412–420 (2018).
35. E. A. Brown, S. P. Day, R. W. Jansen, S. M. Lemon, The 5′ nontranslated region of hepatitis A virus RNA: Secondary structure and elements required for translation in vitro. *J. Virol.* **65**, 5828–5838 (1991).
36. D. Koirala *et al.*, A conserved RNA structural motif for organizing topology within picornaviral internal ribosome entry sites. *Nat. Commun.* **10**, 3629 (2019).
37. E. A. Brown, A. J. Zajac, S. M. Lemon, In vitro characterization of an internal ribosomal entry site (IRES) present within the 5′ nontranslated region of hepatitis A virus RNA: Comparison with the IRES of encephalomyocarditis virus. *J. Virol.* **68**, 1066–1074 (1994).
38. L. A. Passmore, J. Coller, Roles of mRNA poly(A) tails in regulation of eukaryotic gene expression. *Nat. Rev. Mol. Cell Biol.* **23**, 93–106 (2021).
39. X. Han *et al.*, Discovery of RG7834: The first-in-class selective and orally available small molecule hepatitis B virus expression inhibitor with novel mechanism of action. *J. Med. Chem.* **61**, 10619–10634 (2018).
40. J. Herold, R. Andino, Poliovirus RNA replication requires genome circularization through a protein-protein bridge. *Mol. Cell* **7**, 581–591 (2001).
41. P. Friebe, E. Harris, Interplay of RNA elements in the dengue virus 5′ and 3′ ends required for viral RNA replication. *J. Virol.* **84**, 6103–6118 (2010).
42. D. E. Alvarez, M. F. Lodeiro, S. J. Ludueña, L. I. Pietrasanta, A. V. Gamarnik, Long-range RNA-RNA interactions circularize the dengue virus genome. *J. Virol.* **79**, 6631–6643 (2005).
43. I. Frolov, R. Hardy, C. M. Rice, Cis-acting RNA elements at the 5′ end of Sindbis virus genome RNA regulate minus- and plus-strand RNA synthesis. *RNA* **7**, 1638–1651 (2001).
44. A. V. Paul *et al.*, A "slide-back" mechanism for the initiation of protein-primed RNA synthesis by the RNA polymerase of poliovirus. *J. Biol. Chem.* **278**, 43951–43960 (2003).
45. Y. Yang, M. Yi, D. J. Evans, P. Simmonds, S. M. Lemon, Identification of a conserved RNA replication element (cre) within the 3Dpol-coding sequence of hepatoviruses. *J. Virol.* **82**, 10118–10128 (2008).
46. N. Hwang *et al.*, Hepatoselective dihydroquinolizinone Bis-acids for HBsAg mRNA degradation. *ACS Med. Chem. Lett.* **12**, 1130–1136 (2021).
47. N. P. Nelson *et al.*, Prevention of hepatitis A virus infection in the United States: Recommendations of the advisory committee on immunization practices, 2020. *MMWR Recomm. Rep.* **69**, 1–38 (2020).
48. E. L. Van Nostrand *et al.*, Robust transcriptome-wide discovery of RNA-binding protein binding sites with enhanced CLIP (eCLIP). *Nat. Methods* **13**, 508–514 (2016).
49. Y. Li, S. M. Lemon, CLIP-Seq of ZCCHC14 binding sites in HAV-infected cells. Gene Expression Omnibus. https://www.ncbi.nlm.nih.gov/geo/query/acc.cgi?acc=GSE192599. Deposited 3 December 2021.